

Alloy scattering of n -type carriers in $\text{GaN}_x\text{As}_{1-x}$

S. Fahy,¹ A. Lindsay,² H. Ouerdane,^{2,*} and E. P. O'Reilly²

¹*Tyndall National Institute and Department of Physics, University College, Cork, Ireland*

²*Tyndall National Institute, Lee Maltings, Cork, Ireland*

(Received 21 June 2005; revised manuscript received 5 May 2006; published 12 July 2006)

A tight-binding model of the electronic structure of substitutional nitrogen in GaAs, together with a variational description of quasilocalized nitrogen-induced electronic states near the conduction band edge, is used to calculate the nitrogen-related alloy scattering of conduction band electrons in the dilute nitride alloy, $\text{GaN}_x\text{As}_{1-x}$. The electron mobility in the nondegenerate and degenerate doping regimes is calculated for bulk and quantum well geometries from the energy-dependent scattering rate using the Boltzmann transport equation in the relaxation-time approximation. Nitrogen cluster states are found to dominate the scattering near the conduction band edge and play a crucial role in limiting the electron mobility. In the experimentally relevant regime of degenerate doping and at nitrogen concentrations of 1 to 2%, the room-temperature mobility is found to be limited to values less than $300 \text{ cm}^2(\text{V s})^{-1}$, in agreement with experimental measurements.

DOI: [10.1103/PhysRevB.74.035203](https://doi.org/10.1103/PhysRevB.74.035203)

PACS number(s): 72.80.Ey, 72.20.Dp, 71.55.Eq, 72.80.Ng

I. INTRODUCTION

Dilute nitride semiconductor alloys, in particular GaNAs and GaInNAs, have attracted wide attention in the last 5 years,⁴² both for their possible applications in semiconductor laser heterostructures^{1,2} and in high-efficiency solar cells,³ and as prototypical strongly disordered random alloys.⁴⁻⁷ The ability to substantially change the material band gap by the addition of very small concentrations of nitrogen to GaAs and related quaternary alloys,⁸ without significantly changing the lattice parameter of the material, makes them particularly attractive for laser and solar cell applications. The reduction of the band gap is approximately 150 meV for 1% substitutional nitrogen on the group V sites.

However, the addition of these small concentrations of nitrogen to GaAs has also been found to cause a drastic reduction in n -type carrier mobility.⁹⁻¹² For the ternary $\text{GaN}_x\text{As}_{1-x}$ alloys, with x of the order of 0.01, mobilities of less than $200 \text{ cm}^2(\text{V s})^{-1}$ are usually found, although some measurements have shown mobilities as high as $400 \text{ cm}^2(\text{V s})^{-1}$ at low carrier concentrations.¹³ For the quaternary alloy GaInNAs, electron carrier mobilities [typically $<200 \text{ cm}^2(\text{V s})^{-1}$] are also unacceptably low for many applications at present, although some measurements have shown mobilities as high as $2000 \text{ cm}^2(\text{V s})^{-1}$ in Te doped samples.¹⁴

In this paper, we will calculate the effect of localized electronic states, associated with substitutional nitrogen complexes, on the n -type carrier mobility in the dilute nitride $\text{GaAs}_{1-x}\text{N}_x$. We find that such states give rise to strong carrier scattering and a dramatic reduction in carrier mobility. Complexes of more than one substitutional N, sharing Ga nearest neighbors, are found to give rise to particularly strong scattering and limit the room temperature mobility to less than $300 \text{ cm}^2(\text{V s})^{-1}$ for carrier concentrations of the order of 10^{18} cm^{-3} when the substitutional nitrogen concentration is in the range 1 to 2%.

A simple, physical understanding of the dramatic effect of substitutional nitrogen on the band gap of GaAs has been based on the band anticrossing model developed by Shan *et al.*¹⁵ They used hydrostatic pressure techniques to show

that the reduction in energy gap can be described by an interaction between the conduction band edge and a higher-lying set of localized nitrogen resonant states. In the ideal case, nitrogen substitutes onto As sites in GaAs (or GaInAs). Although nitrogen is isoelectronic with arsenic, because of the large difference in size and electronegativity between nitrogen and arsenic atoms, this causes the formation of quasilocalized electron states associated with the substitutional nitrogen atoms,^{16,17} which interact strongly with the GaAs conduction band edge. This leads to several effects: (a) substantial reduction of the band gap at nitrogen concentrations of a few percent;^{5,8,15,18,19} (b) a marked increase in the conduction band edge effective mass, which has a nonmonotonic composition dependence;^{7,20} and (c) a dramatic increase in carrier scattering and an associated reduction in the carrier mobility for electrons in the materials.^{6,9-12,21-23}

In Ref. 5, Kent and Zunger have used empirical pseudopotential methods, applied to large supercells, to provide an extensive study of the formation of cluster states near the conduction edge in dilute nitrides. In a generalization of the band anticrossing model,⁷ using tight-binding methods to include the interaction between localized nitrogen states in the dilute alloy, we have obtained similar results on the formation of nitrogen cluster states, with energies near the conduction band edge, which hybridize strongly with the GaAs conduction band-edge states. We demonstrated that cluster states have a very substantial effect on the effective mass near the band edge.^{7,20}

In an earlier paper,⁶ we have also shown that the local band-edge fluctuations²⁴ due to the interaction with localized states associated with isolated nitrogen substitutional atoms leads to a reduction of the n -type mobility in dilute nitrides to values of the order of $1000\text{--}2000 \text{ cm}^2(\text{V s})^{-1}$. This is a significant reduction compared to the room temperature mobility of order $8000 \text{ cm}^2(\text{V s})^{-1}$ in GaAs but is still not sufficient to account for the extremely low measured mobilities in $\text{GaN}_x\text{As}_{1-x}$. In the present work, we will extend this study to include the interaction of the conduction band with the full range of nitrogen-related cluster states. We represent these localized states near the conduction band edge and calculate

their interaction with the carrier states in a variational tight-binding representation, where all states are expressed as a linear combination of localized states, centered on the individual nitrogen atoms.⁷ We consider resonant scattering by the localized states in the system, generalizing early investigations²¹ of the effect of resonant scattering of carriers by a single type of localized state and find the carrier mobility by solving the Boltzmann transport equation in the relaxation time approximation. Fisher *et al.*²⁵ have measured the resonant scattering of carriers in AlGaAs by Si defects, using pressure to shift the resonant localized state associated with Si relative to the band edge, and accounted quantitatively for the observed dip in mobility as the Fermi level passed through the single resonant state energy.

Nonsubstitutional defects have been studied by Zhang *et al.*^{26,27} using density functional theory methods, showing that nitrogen split interstitials and other nonsubstitutional nitrogen defects may be a significant cause of charge trapping in these materials. Such trapped charge centers may lead to substantial further reduction in carrier mobility.

In the present work, we treat the effects of substitutional nitrogen only, without considering any interstitial defects or charge trapping. Preliminary work along these lines has been reported in Ref. 23 for nondegenerate doping levels. Here, we give details of the full formalism required for this approach and report results for bulk and two-dimensional mobilities for degenerate and nondegenerate carrier concentrations. Carrier mobilities are found to be reduced considerably in degenerately doped samples, due to the increased interaction of conduction band states with the localized, nitrogen-related states as one increases the energy from the band edge. Carrier mobility in quantum well structures is found to be comparable to that in bulk.

The rest of the paper is organized as follows: in Sec. II A, we discuss the model of localized nitrogen-related states and their numerical representation. In Secs. II B and II C, we review the theory of resonant scattering by a single localized state in three-dimensional and two-dimensional systems. In Sec. II D, we consider the combined effect of many, randomly placed, resonant scatterers and discuss the effects of the average renormalization of the band states through hybridization with localized states. In Sec. II E, we derive the expressions required to evaluate the mobility from the Boltzmann transport equation in the relaxation time approximation, using the energy-dependent scattering rates due to interaction with multiple types of scattering centers. We present the numerical results of applying the methods to GaNAs for nitrogen concentrations up to 2% in Sec. III and discuss the overall conclusions of our study in Sec. IV.

II. MODEL OF SCATTERING AND MOBILITY

A. Quasilocalized nitrogen cluster electronic states

Substitutional nitrogen strongly perturbs the conduction bands of GaAs in the alloy $\text{GaN}_x\text{As}_{1-x}$ and produces a range of quasilocalized electronic states due to the incorporated nitrogen atoms.^{4,7} When these states have energies within the conduction band, they form resonances. When they lie within the energy band gap, they are strictly localized. In either

case, the state can be viewed in a first approximation as localized, made up from states throughout the Brillouin zone of the host material.¹⁶ This state then hybridizes with the extended GaAs states near the conduction band edge.^{4,15,28} The perturbation of extended states, which are resonant or near resonant with the quasilocalized levels, is strong, leading to a high scattering rate of carriers in those states. This picture of the formation of states associated with a single substitutional nitrogen (as linear combinations of a single, localized, *energy-independent* state $|N\rangle$ and the conduction band states $|p\rangle$) is incorporated in the band anticrossing model¹⁵ and is fully substantiated in the ultradilute limit by tight-binding calculations which include conduction band states throughout the Brillouin zone on an equal footing.²⁹ This picture is also supported by direct experimental measurement of the band dispersion using magnetotunneling spectroscopy in an ultradilute GaNAs quantum well.³⁰

The validity of this description of the low-lying conduction band states in the dilute alloy (within 200 meV of the conduction band edge) depends on both the strongly electronegative character and small size of nitrogen (compared to As, for which it substitutes) and the low density of states near the conduction band edge at Γ in GaAs. Except for a small region near the Γ -point in the Brillouin zone, where the energy bands dip to the conduction band minimum, the principal weight of the density of states in the GaAs conduction bands lies above the L-point minimum. The small effective mass at the Γ -point minimum in GaAs implies that the density of states is much lower near the band edge than above the L-point energy.

In considering the effect of the strong nitrogen perturbation on these conduction bands, we can, as a first approximation, neglect the low density of states below the L-point minimum.³¹ The electronegative interaction and small size of the nitrogen then create a “bound state” $|N\rangle$ (i.e., a state below the L-point conduction band minimum) which is localized about the nitrogen atom.¹⁶ It lies approximately 100 meV below the L-point conduction band minimum^{17,29} and is a linear combination of states from throughout the GaAs Brillouin zone (but principally around the L-point and to a lesser extent around the X-point).⁴

We then consider the interaction of this localized state (in a lattice of N_a GaAs primitive unit cells) with the conduction band states $|p\rangle$, previously neglected, near the Γ -point minimum. The interaction matrix element with these states is relatively insensitive to energy since the state $|N\rangle$ is highly localized, compared to the de Broglie wavelength of such states. (Taking the normalization of the extended states $|p\rangle$ into account, we see that this matrix element is proportional to $1/\sqrt{N_a}$ and denote it by $\beta/\sqrt{N_a}$, where β is a material constant.³² In practice, $\beta \approx 2.5$ eV for substitutional nitrogen in GaAs.) When the conduction band state is resonant with the localized state, a large hybridization occurs between them. The eigenstates $|p'\rangle$ of the full Hamiltonian can be written as $|p'\rangle = \langle N|p'\rangle|N\rangle + \sum_p \langle p|p'\rangle|p\rangle$. Since the density of conduction band states is small at the energy of the localized state (due to the small effective mass in the conduction band), the resonance width of the localized state (i.e., the range of energy over which $|\langle p'|N\rangle|^2$ is substantial) is narrow (of the order of 20 meV).

When many substitutional nitrogen atoms are present in the ultradilute alloy, the low-lying states in the conduction band can be approximately represented as linear combinations of the localized states associated with each nitrogen site and the GaAs conduction band states. The linear combination of isolated nitrogen states (LCINS) approach⁷ has been developed to extend this description to alloys with substitutional nitrogen at concentrations of up to several atomic percent.

Parameterized tight-binding calculations of GaAsN give an excellent description of the low-lying conduction band states of the alloy. They can be applied directly in calculations involving several hundred GaAs unit cells. However, in order to study the range of states induced by random substitutional nitrogen near the conduction band minimum, including those associated with random clusters of nitrogen, one needs to study the alloy on a longer length scale, requiring calculations of up to 10^7 unit cells. A direct tight-binding approach to such problems is not numerically feasible. However, the LCINS approach uses the character of the nitrogen-induced quasilocated states to give a compact representation of the states near the conduction band edge in terms of a much smaller basis set of states: (1) states associated with a single isolated nitrogen substitutional impurity in GaAs, (2) when several nitrogen atoms (2–4 nitrogen atoms) share a common Ga nearest neighbor, the bonding combination of states for that cluster of atoms (otherwise isolated in the GaAs host lattice) is included, and (3) GaAs conduction band states $|p\rangle$. The states in (1) and (2) are determined in a tight-binding calculation for a supercell (i.e., a parallelepiped region on which we will impose periodic boundary conditions) of several hundred GaAs unit cells, with one substitutional nitrogen atom for (1) or with 2, 3, or 4 nitrogen atoms for (2). In either case (1) or (2), the lowest eigenstate $|\psi\rangle$ near the conduction band edge is calculated by diagonalization of the tight-binding Hamiltonian. The localized nitrogen (or nitrogen cluster) state $|L\rangle$ is then defined by subtracting the component of the pure GaAs conduction band $|p\rangle$ from $|\psi\rangle$, as follows:

$$|L\rangle = \frac{|\psi\rangle - |p\rangle\langle p|\psi\rangle}{\sqrt{1 - |\langle p|\psi\rangle|^2}}. \quad (1)$$

The states $|L\rangle$ are calculated to be largely concentrated on the first two shells of atoms around the nitrogen site in case (1) or the shared Ga nearest-neighbor site in case (2).

A large supercell, containing N_a primitive zinc-blende unit cells, is used to represent a volume of the random alloy. (In the calculations presented in Sec. III, below, N_a will typically be between 10^5 and 10^7 .) Nitrogen atoms are distributed randomly on the group V sites: at each group V site, we place a nitrogen atom, with probability x , or else an arsenic atom. The choice of atom on each group V site is independent of the choice on other sites, so that no preferential clustering of nitrogen is included. However, complexes of two or more nitrogen sites sharing gallium nearest neighbors are formed at random in the system. (These will prove to be important in determining the transport properties of the material.) For a given distribution of nitrogen atoms on the

group V sites, localized cluster states are expanded as linear combinations of the basis states, $|L_i\rangle$, one centered on each nitrogen site in the case (1) of the isolated nitrogen atoms, or centered on the shared Ga nearest neighbor for each nitrogen cluster in the case (2). A reduced Hamiltonian

$$H_{ij}^{\text{red}} = \langle L_i|H^{TB}|L_j\rangle, \quad (2)$$

where H^{TB} is the full tight-binding Hamiltonian, is calculated. The eigenstates $|N_j\rangle = \sum_i c_{ij}|L_i\rangle$ and eigenvalues $E_{N,j}$ of H^{red} are found by numerical solution of the eigenvalue equation,

$$\sum_l H_{il}^{\text{red}} c_{lj} = E_{N,j} \sum_l S_{il} c_{lj}, \quad (3)$$

where we include the overlap matrix elements $S_{ij} = \langle L_i|L_j\rangle$ to reflect that neighboring N localized states are not normally orthogonal to each other. The matrix elements,

$$\langle N_j|H^{TB}|p\rangle = H_{j0}^{\text{red}} = \beta_j/\sqrt{N_a}, \quad (4)$$

with the conduction band-edge state $|p\rangle$ are also calculated from the full, tight-binding representation of $|N_j\rangle$ and $|p\rangle$.

The energy of the conduction band edge in the alloy can be found by diagonalizing the reduced Hamiltonian, including the interaction with the GaAs conduction band edge. The new conduction band-edge state $|c\rangle$ is then found by identifying that eigenstate (energy E_c) which has maximal overlap $|\langle p|c\rangle|^2$ with the original GaAs conduction band-edge state (energy E_p). The ratio of the GaAs effective mass to the alloy effective mass is then given by

$$\frac{m_0^*}{m^*} = \frac{dE_c}{dE_p} = |\langle p|c\rangle|^2 \equiv f_\Gamma. \quad (5)$$

(We note that, in treating the conduction bands only, we do not include here the additional, relatively small change in the effective mass arising from interaction with the valence band.⁷ This change is approximately proportional to the band gap E_g in $\mathbf{k}\cdot\mathbf{p}$ theory.) It is significant that, even in supercells containing of the order of 10^4 localized nitrogen-related states, f_Γ remains of the order of unity, demonstrating that the band states retain their itinerant character in the alloy.⁷

Previous calculations²⁹ using the LCINS representation of electron states near the conduction band edge for medium-sized supercells containing a variety of substitutional nitrogen environments (random distribution of nitrogen atoms, clusters of up to four nitrogen atoms, etc.) have demonstrated close agreement with the corresponding full tight-binding calculations, both in the eigenvalues and in the weight $f_\Gamma \equiv |\langle p|\psi\rangle|^2$ of the GaAs conduction band state $|p\rangle$ in the eigenstates of the reduced Hamiltonian H^{red} . Moreover, the effective mass, obtained from the value of f_Γ in very large supercells, is in good agreement with experimental values for various nitrogen concentrations in the range 0.1–2.0%.⁷ The observed nonmonotonic variation in the low-temperature effective mass for $x < 0.4\%$ has in particular been correlated with interactions with specific N pair and triplet states identified in photoluminescence measurements close to the conduction band edge.²⁰

For s -wave scattering, the shift in energy on the introduction of a defect is directly proportional to the scattering matrix element $\langle \psi | H - H_0 | p \rangle = \langle \psi | \Delta H | p \rangle$, where H is the Hamiltonian with the nitrogen atoms present and H_0 is the Hamiltonian for the ideal periodic host.⁶ Moreover, the energy derivative of the scattering matrix element is proportional to f_Γ .²³ Therefore the matching of eigenvalues and f_Γ between H^{red} and the full tight-binding Hamiltonian H^{TB} ensures that the scattering cross section of the nitrogen atoms and clusters for carriers close to the conduction band edge is correctly given by the reduced Hamiltonian H^{red} . (We note that this is the same basic concept as is applied in defining transferrable *ab initio* atomic pseudopotentials, widely used in electronic structure theory calculations.³³)

B. Resonant scattering by a single quasilocalized state

In the independent scattering approximation, the total scattering rate due to randomly placed localized states, coupling weakly to the conduction band states, is the sum of the scattering rates of the individual sites. This approximation assumes that the states do not interact significantly with each other, either through interaction matrix elements in the single-particle Hamiltonian, or in statistical correlation between their occurrence and locations in the material.

The former assumption is justified in considering scattering from the states $|N_j\rangle$ because these states have been constructed by diagonalization of the LCINS Hamiltonian (i.e., explicitly so that Hamiltonian matrix elements between the localized states are zero). We note that this is *not* the same as assuming that each nitrogen substitutional atom contributes independently to scattering; hybridization between nitrogen states is taken into account. [This is in contrast to the coherent potential approximation (CPA), where no interaction between nitrogen sites is taken into account.³⁴] However, we are assuming that only one localized state associated with each cluster of nitrogen atoms contributes significantly to the scattering of a given conduction band state and that, when a cluster is added or removed, the only change in the scattering is due to the removal or addition of a single localized state.

The lack of statistical correlation between clusters is approximately true because of the low density of cluster states. Although the existence of a cluster, occupying certain sites of the solid, excludes the possibility of other N atoms or clusters on those sites, the overall density of clusters (or single nitrogen sites) is sufficiently low that this exclusion should have only a small effect.

In preparing the N atomic distribution at each composition x we assume a fully random distribution of N atoms, by placing a N atom with probability x on each group-V site, ignoring any preferential clustering which might be expected if the crystal energy were in a global minimum. The growth of GaNAs alloys occurs away from equilibrium, so that the distribution of N atoms is more likely to be random rather than associated with the lowest energy configuration. We regard the use of a fully random distribution of N atoms as the best first approximation. This is supported by scanning tunneling microscopy studies³⁵ of the arrangement of nitrogen atoms in GaAsN alloys and by the observed evolution of N

pairs and larger clusters in photoluminescence and magneto-spectroscopy experiments.^{20,30,36}

First we consider a single localized state, located at the origin, $\mathbf{r}=0$, interacting with a continuum of conduction band states. In the absence of the interaction between conduction band states and localized state, the Hamiltonian is

$$H_0 = E_N |N\rangle\langle N| + \sum_p E(p) |p\rangle\langle p|, \quad (6)$$

where p now labels the conduction band momentum, $E(p) = E_c + \frac{p^2}{2m^*}$, $|N\rangle$ is the localized state and E_N its energy. The Hamiltonian perturbation ΔH , due to the interaction of the localized state with the conduction band, is

$$\Delta H = \sum_p \frac{\beta}{\sqrt{N_a}} [|p\rangle\langle N| + |N\rangle\langle p|], \quad (7)$$

where N_a is the number of group-V atoms in the system and β defines the interaction strength. Since the state $|N\rangle$ is highly localized and we consider GaAs band states $|p\rangle$ only near the zone center, we assume that this interaction strength is independent of the momentum of the conduction band state. The energy E_N of the localized state and its interaction matrix element with the GaAs conduction band near the Γ -point has already been calculated within the LCINS representation. (For many of the nitrogen-related localized states in GaAs, β is of the order of 2 eV.) Assuming a parabolic band, with energy $E = p^2/2m^*$, the density of states for conduction band states (one spin direction only) is

$$\begin{aligned} D(E) &= \frac{\text{volume}}{4\pi^2 \hbar^3} 2m^* \sqrt{2m^* E} = \frac{N_a (a_0^3/4)}{4\pi^2 \hbar^3} 2m^* \sqrt{2m^* E} \\ &= \frac{N_a}{16\pi^2 E_0} \sqrt{\frac{E}{E_0}}, \end{aligned} \quad (8)$$

where $E_0 = \hbar^2/(2m^* a_0^2)$ and a_0 is the cubic lattice constant. (For the GaAs conduction band, with effective mass $m^* = 0.067m$, $E_0 = 1.781$ eV.)

Due to the interaction with the conduction band states, the localized state has a finite lifetime and broadens into a resonance (quasilocalized state).^{16,21,25} From Fermi's "golden rule," the decay rate of the state $|N\rangle$ is given by

$$R_N = \frac{2\pi}{\hbar} |\langle p | \Delta H | N \rangle|^2 D(E_N) = \frac{2\pi}{\hbar} \beta^2 \frac{D(E_N)}{N_a} = \Gamma/\hbar. \quad (9)$$

This gives a time-dependent wave function $|\psi\rangle$ with $\langle N | \psi(t) \rangle \approx \exp[-i(E'_N - i\Gamma/2)t/\hbar]$, where the energy may be shifted by the interaction ΔH to a new value E'_N . Taking the Fourier transform of this gives a Lorentzian line shape for the weight of the localized state $|N\rangle$,

$$|\langle p' | N \rangle|^2 \approx \frac{C}{[E(p') - E'_N]^2 + (\Gamma/2)^2}, \quad (10)$$

where $|p'\rangle$ denotes the exact eigenstate of $H_0 + \Delta H$ which has largest overlap with the momentum eigenstate $|p\rangle$ and C is a normalization constant, chosen to ensure that $\int |\langle p' | N \rangle|^2 D[E(p')] dE(p') \equiv \langle N | N \rangle = 1$. When the density of states is approximately constant, $D[E(p')] \approx D(E_N)$, over the

peak of the Lorentzian, one can then obtain that $C = \beta^2/N_a$. The energy shift $E_N - E'_N$ and linewidth Γ can be determined more generally by sum rules, even when the conduction band density of states is not constant, as discussed in detail in Appendix A.

To find the scattering rate of conduction band carriers due to their interaction with the localized state $|N\rangle$, we need the scattering matrix element $S(p, p') = \langle p|H|p'\rangle$ between bare conduction band states $|p\rangle$ and dressed states $|p'\rangle$. For the interaction ΔH this is exactly $S(p, p') = \langle N|p'\rangle\beta/\sqrt{N_a}$. Within the Lorentzian approximation for the line shape, given in Eq. (10), the scattering rate for carriers of energy E is then

$$R(E) = \frac{2\pi}{\hbar} |S(p, p')|^2 D(E) = \frac{2\pi}{\hbar N_a} \frac{\beta^4}{(E - E'_N)^2 + (\Gamma/2)^2} \frac{D(E)}{N_a}. \quad (11)$$

This is an analytic continuation of the result for scattering from a localized state which is nonresonant, replacing E'_N with the complex energy $E'_N - i(\Gamma/2)$, obtained from the expression for the time dependence of $\langle N|\psi\rangle$, where $\Gamma/2 = \pi\beta^2 D(E'_N)/N_a$ is the imaginary part of the energy. Since $S(p, p')$ does not depend on $|p - p'|$, the scattering is isotropic in this model.

C. Carrier scattering in quantum wells

For carrier scattering in quantum well structures, a similar analysis applies to that given above for the bulk. The quantum well has area A and thickness d , and we assume the substitutional nitrogen is distributed on the N_a group V sites in a homogeneous statistical distribution throughout the well. The localized states $|L_i\rangle$ are statistically of the same character as those of the bulk at the same nitrogen concentration, since they are unaffected by the quantum well boundary conditions. (For simplicity, we are neglecting any effects of epitaxial strain, which may cause a relative shift of the localized state and conduction band edge energies.) We restrict our analysis to carriers in the lowest quantum well subband. In the effective mass approximation, the extended, bare GaAs conduction band states of the bulk are now replaced by states (in the lowest quantum well subband) of the form:

$$\psi_p(x, y, z) = \frac{1}{\sqrt{A}} \exp[i(p_x x + p_y y)] \Psi(z), \quad (12)$$

where $\Psi(z)$ is the transverse wave function within the well. In practice this function is not identically zero outside the well^{37,38} but, for simplicity, we will assume that the barrier regions completely confine the electrons in the quantum well region, $0 < z < d$. Then the transverse wave function is

$$\Psi(z) = \sqrt{\frac{2}{d}} \sin\left(\frac{\pi z}{d}\right). \quad (13)$$

To treat the scattering of carriers in a quantum well by a single defect state $|N\rangle$ at a position $\mathbf{r} = (x, y, z)$, it is convenient to rewrite the scattering Hamiltonian in Eq. (7) in an equivalent form as

$$\Delta H = \beta \frac{a_0^3}{4} [|\mathbf{r}\rangle\langle N| + |N\rangle\langle \mathbf{r}|], \quad (14)$$

where $a_0^3/4$ is the volume of a single zinc-blende primitive unit cell and $|\mathbf{r}\rangle$ is the coordinate eigenstate from the GaAs effective mass conduction band states [so that $\langle \mathbf{r}|\psi\rangle = \psi_{\text{em}}(\mathbf{r})$, where $\psi_{\text{em}}(\mathbf{r})$ is the GaAs conduction band component of the state $|\psi\rangle$ at the position \mathbf{r}]. The analysis of the resonance width of the state $|N\rangle$ in the quantum well is similar to that in the bulk, with the interaction parameter β replaced by $\beta\Psi(z)$ and the bulk density of states $D(E)$ replaced by the two-dimensional density of states $D_{QW}(E) = Am^*/(2\pi\hbar^2)$ for $E > E_c$. The conduction band edge E_c is raised above the bulk value, due to the transverse confinement kinetic energy, by approximately

$$dE = \frac{\hbar^2}{2m^*} \left(\frac{\pi}{d}\right)^2. \quad (15)$$

Incomplete wave function confinement in the quantum well will reduce the value of dE , but we neglect this effect. (We also neglect the more complicated effects of quantum well confinement on higher quantum well subbands in the band anticrossing model, discussed in Ref. 37, since we are interested only in the lowest subband and only in states near the edge of that subband.) This gives a scattering rate of

$$\begin{aligned} R_{QW}(E) &= \frac{2\pi}{\hbar} |S(p, p')|^2 D_{QW}(E) \\ &= \frac{2\pi}{\hbar N_a} \frac{\beta^4 \Psi(z)^4 d}{(E - E'_N)^2 + (\Gamma/2)^2} \frac{a_0^3 D_{QW}(E)}{4A}, \end{aligned} \quad (16)$$

where the localized state linewidth is given by

$$\begin{aligned} \Gamma &= 2\pi \frac{|\Psi(z)|^2 a_0^3}{A} \frac{\beta^2 D_{QW}(E)}{4} \\ &= 2\pi \frac{2 \sin^2(\pi z/d) a_0^3}{Ad} \frac{\beta^2 Am^*}{4 \cdot 2\pi\hbar^2} \quad \text{for } E'_N > E_c. \end{aligned} \quad (17)$$

For $E'_N < E_c$, $\Gamma = 0$. Since the distribution of nitrogen sites is assumed to be uniform within the well, we replace the factor $\Psi(z)^4$ with its average value, $3/(2d^2)$, leading to an approximate expression for the scattering rate:⁴³

$$R_{QW}(E) = \frac{3\pi}{\hbar N_a} \frac{\beta^4}{(E - E'_N)^2 + (\Gamma_{av}/2)^2} \frac{a_0^3 m^*}{8d\pi\hbar^2}, \quad (18)$$

where $\Gamma_{av} = 0$ for $E'_N < E_c$ and

$$\Gamma_{av} \equiv 2\pi \sqrt{\frac{3}{2}} \beta^2 \frac{a_0^3 m^*}{8d\pi\hbar^2} \quad \text{for } E'_N > E_c. \quad (19)$$

D. Multiple localized states

There are many nitrogen-induced scattering centers of various types (single-N, N-N pairs, larger clusters, etc.) distributed randomly throughout the material.⁷ We will assume that each of these scattering centers corresponds to a single, localized state $|N_i\rangle$, obtained from diagonalization of the lo-

calized part of H^{red} , as discussed in Sec. II A, above. (For a cluster containing more than two nitrogen atoms, there will be more than one LCINS state concentrated on that cluster but the phase combination of LCINS orbitals leads to very small interaction matrix elements with the conduction band for all except one of those states.) Interaction between cluster states is assumed to be very weak (by definition of a cluster), giving rise to an inhomogeneous broadening of the localized state energy for each cluster due to its environment and the other nitrogen atoms nearby. This is reflected in the spectrum of localized states found by diagonalization of the localized part of the LCINS reduced Hamiltonian, H_{ij}^{red} for $i, j > 0$, where one finds many almost degenerate states at energies corresponding to the energy of, for example, isolated N atoms or second nearest-neighbor N-N pairs.

In calculating the appropriate matrix elements $\beta/\sqrt{N_a}$ for scattering by individual clusters from the eigenstates $|N_j\rangle$ of the localized part of H^{red} , a difficulty arises from the weak coupling of almost degenerate cluster states: two identical localized cluster states will hybridize into symmetric and antisymmetric linear combinations, even if their interaction is infinitesimally weak, giving rise to one state with a coupling $\sqrt{2}$ times the single cluster interaction and another with zero coupling to the conduction bands. When this is used in the calculation of scattering, the cross section is proportional to β^4 and so the scattering calculated, considering the hybridized states as independent scatterers, is twice what one would obtain without the hybridization. This result is not physically correct, because the two clusters in the material are statistically independent and their scattering intensities, rather than their amplitudes, should be added.

Interactions between many such physically identical clusters in the alloy give rise to states $|N_j\rangle$ with energies very close to each other, but with a wide range of conduction band interaction matrix elements due to random hybridization between the states on the various clusters. To approximate the physically correct result (which takes each cluster's independent contribution to the scattered wave intensity), we average β^2 (the square of the matrix element between the localized state and the conduction band) for all localized states with energies over a small energy window (of width about 1 meV). We then assume that one localized state corresponds to each physically separate cluster and that all cluster states within that window have the same value of β^2 , equal to the average of β^2 over the hybridized states within the energy window. We find that the width of the energy window, within the range 0.5–5.0 meV, has only a very weak effect on the final calculated mobility.

Hybridization of the conduction band with all localized states in the alloy leads to a reduction of the weight of the GaAs conduction band in the alloy conduction band states by the factor f_Γ . To obtain the contribution of each localized state $|N_j\rangle$ to the scattering of conduction states, we must consider its interaction with the conduction states in the alloy, which are linear combinations of the original GaAs conduction band states and the other localized states in the system:

$$|c\rangle = \sum_p \langle p|c\rangle|p\rangle + \sum_{j \neq i} A_j |N_j\rangle, \quad (20)$$

where $|A_j|^2 = W_j(E)$ is the weight of the localized state j in the exact states of the system at energy E . If momentum

conservation is still a reasonably good approximation, the conduction band weights $|\langle p|c\rangle|^2$ will be concentrated on a single value of p for each state c , or at least in a very small range of energies. The total sum of conduction band state weights is

$$f_\Gamma = \sum_p |\langle p|c\rangle|^2 = 1 - \sum_i W_i(E). \quad (21)$$

In such a system, each individual localized state interacts with these delocalized states $|c\rangle$, which are linear combinations of conduction band states and the other localized states. Since localized states couple directly only to the GaAs conduction band states $|p\rangle$, the interaction matrix element with $|c\rangle$ is reduced to $\beta^2 f_\Gamma$. However, the density of states is increased by a factor of

$$\frac{dE}{dE(p)} = f_\Gamma. \quad (22)$$

In summary, we treat the carrier scattering rate by multiple, independent localized states as a sum of the rates from individual localized states, but allow for the change in effective matrix element $(\beta')^2 = \beta^2 f_\Gamma$ and effective mass, $m^* = m_0^*/f_\Gamma$, of delocalized band states, which corresponds to the change in density of states $D'(E') = D(E)/f_\Gamma$, where E' is the energy of the alloy state of momentum \mathbf{p} and E is the energy of the corresponding GaAs state. Values for E_c and f_Γ are taken from the diagonalizations of H^{red} for very large supercells in the LCINS representation and f_Γ is assumed to be energy independent (within several kT of the conduction band edge). The total scattering rate $R(E)$ at energy E is then the sum of the individual scattering rates $R_j(E)$ for each state $|N_j\rangle$, as given in Eq. (11) or, in the case of quantum wells, Eq. (18).

We emphasize that, although the large supercells used to construct the localized state spectrum are formally periodic, their size is sufficient that this has a negligible effect on the localized states calculated and on the overall spectrum. Moreover, our assumption that the total scattering rate $R(E)$ at energy E is the sum of the scattering rates from the individual localized states supposes that the localized states are randomly distributed. Our calculation of the energy-dependent scattering rate by each localized state (Sec. II B) assumes that it is located in an infinite system with a continuous density of carrier states.

The approach of resonant scattering by a single type of scatterer is closely related to the CPA.³⁴ In the low alloy concentration limit (as in the dilute nitrides) the two approaches give identical results if the single-site scattering problem is treated in the same way. (We note that the approximate solution of the CPA given in Ref. 34 assumes that the density of carrier states is independent of energy, which is reasonably close to the localized state energy but is not appropriate for carriers at the band edge. Our result, Eq. (11), for the single-state scattering rate does not make this assumption.) If T is the scattering T-matrix³⁹ of a single scatterer in a unit volume, then for a concentration x of such scattering centers (neglecting terms of order x^2) the CPA gives the self-energy shift $\Delta E_{\mathbf{k}_n}$ of states of momentum \mathbf{k} in

band n as $x\langle\mathbf{k}_n|T|\mathbf{k}_n\rangle$, where $|\mathbf{k}_n\rangle$ is the state of momentum \mathbf{k} which diagonalizes $E_{\mathbf{k}n}\delta_{mn}+x\langle\mathbf{k}_m|T|\mathbf{k}_n\rangle$. From the optical theorem,³⁹ the scattering rate calculated in the resonant scattering approach is the same as the imaginary part of the self-energy (scaled by $2/\hbar$) in the exact CPA. The present approach reduces to that of Ref. 6 when both (a) the interaction between nitrogen-induced localized states is neglected and (b) the carriers are at energy E such that $|E-E_j|\gg\Gamma_j$; for the dilute nitrides, if condition (a) applies, then condition (b) is satisfied for carriers near the band edge since Γ for the isolated nitrogen state is approximately 25 meV and $E_N-E_c\approx 180$ meV.

The more general treatment presented in this section may be thought of intuitively as a generalization of the CPA, where we allow for many types of scattering centers (i.e., the various nitrogen pair and cluster states), using the calculation of states in the supercell to obtain the coupled mean-field carrier wave function and the real-part of the self-energy shift. The imaginary part of the band self-energy is obtained from the calculation of resonant scattering of the mean-field states. The modification of the scattering matrix element, from β to $\beta'=\beta\sqrt{f_\Gamma}$, gives a self-consistent treatment of the scattering and the mean-field wave function.

E. Carrier mobility from the Boltzmann transport equation

In the relaxation time approximation, the Boltzmann transport equation gives the following result⁴⁰ for the current density due to an electric field \mathcal{E} :

$$\mathbf{j} = -\frac{2e^2}{(2\pi\hbar)^3} \int \frac{1}{R[E(\mathbf{p})]} \mathcal{E} \cdot \nabla_{\mathbf{p}} f_0(\mathbf{p}) \mathbf{v}(\mathbf{p}) d^3\mathbf{p}, \quad (23)$$

where $R(E)$ is the relaxation rate for the distribution at energy E (which we set equal to the alloy carrier scattering rate, discussed in Sec. II D), f_0 is the thermal (Fermi-Dirac) distribution of carriers in the states, \mathbf{p} is the momentum label of the states, and $\mathbf{v}(\mathbf{p})=\nabla_{\mathbf{p}}E(\mathbf{p})$ is the carrier velocity for momentum \mathbf{p} . Assuming a parabolic energy dispersion, $E(p)=E_c+p^2/2m^*$, near the band minimum, the current density for an isotropic material can then be rewritten as

$$j = -\frac{2e^2\mathcal{E}}{3(2\pi\hbar)^3} \int_0^\infty \frac{p^2}{m^*R(E)} \frac{\partial f_0}{\partial E} 4\pi p^2 dp. \quad (24)$$

The carrier mobility is given by

$$\mu = \frac{j}{en\mathcal{E}}, \quad (25)$$

where the density of carriers,

$$n = \frac{2}{(2\pi\hbar)^3} \int_0^\infty f_0[E(p)] 4\pi p^2 dp. \quad (26)$$

For nondegenerate carrier concentrations ($n\leq 10^{16}$ cm⁻³), we may use the Maxwell-Boltzmann distribution, $f_0(E)=\exp[(E_F-E)/kT]$. In this case an analytic expression can be found for the carrier concentration:

$$n = 2 \exp[E_F - E_c] \left\{ \frac{m^* kT}{2\pi\hbar^2} \right\}^{3/2}. \quad (27)$$

Transforming the integrals over p to integrals over u , where $u^2=p^2/(2m^*kT)$, then gives the mobility

$$\mu = \frac{e4\sqrt{2}}{3\sqrt{\pi m^* kT}} \left(\frac{2\pi\hbar^2}{m^*} \right)^2 \frac{1}{\pi a_0^3} \int \frac{e^{-u^2} u^3 du}{M(kTu^2)}, \quad (28)$$

where

$$M(E) = \frac{1}{N_a} \sum_i \frac{\beta_i'^4}{(E_c + E - E_i)^2 + (\Gamma_i/2)^2}. \quad (29)$$

This integral can be evaluated numerically for a given distribution of localized states.

In the degenerate regime, the full form of the Fermi-Dirac distribution, $f_0(E)=\{\exp[(E-E_F)/kT]+1\}^{-1}$, is used. As expected, due to the derivative $\partial f_0/\partial E$ of the distribution function, appearing in Eq. (24), the states within kT of the Fermi level E_F dominate the current. In the degenerate regime, we evaluate both Eqs. (24) and (26) by numerical integration and find the mobility from Eq. (25).

For the quantum well case, we replace the three-dimensional expressions for the current and carrier density in Eqs. (24) and (26), respectively, with the corresponding two-dimensional expressions,

$$j_{QW} = -\frac{e^2\mathcal{E}}{(2\pi\hbar)^2} \int_0^\infty \frac{p^2}{m^*R_{QW}(E)} \frac{\partial f_0}{\partial E} 2\pi p dp, \quad (30)$$

where R_{QW} is the scattering rate in the quantum well, as given in Eq. (18) with $m^*=m_0^*/f_\Gamma$ and $\beta'=\beta\sqrt{f_\Gamma}$, and

$$\begin{aligned} n_{QW} &= \frac{2}{(2\pi\hbar)^2} \int_0^\infty f_0[E(p)] 2\pi p dp \\ &= \frac{m^* kT}{\pi\hbar^2} \ln \left[1 + \exp\left(\frac{E_F - E_{c,QW}}{kT}\right) \right], \end{aligned} \quad (31)$$

where we have used the explicit form of the Fermi-Dirac distribution in the second part of the equation for the carrier concentration. The band edge $E_{c,QW}$ is shifted by confinement, as given in Eq. (15). Substituting the full form of the expressions in Eqs. (18), (30), and (31) into Eq. (25) gives

$$\mu = \frac{16ed\hbar^3}{3m^*a_0^3} \frac{1}{\ln[1+e^\eta]} \int_0^\infty \frac{e^{u^2-\eta} u^3 du}{M_{QW}(kTu^2)[e^{u^2-\eta}+1]^2}, \quad (32)$$

where $\eta=(E_F-E_{c,QW})/kT$, and

$$M_{QW}(E) = \frac{1}{N_a} \sum_i \frac{\beta_i'^4}{(E_{c,QW} + E - E_i)^2 + (\Gamma_{av,i}/2)^2}. \quad (33)$$

In the nondegenerate limit ($\eta\rightarrow-\infty$), this reduces to

$$\mu = \frac{16ed\hbar^3}{3m^*a_0^3} \int_0^\infty \frac{e^{-u^2} u^3 du}{M_{QW}(kTu^2)}. \quad (34)$$

TABLE I. Details of the supercells used to calculate the LCINS localized states for various values of the nitrogen concentration x . N_a is the number of zinc-blende primitive unit cells in the supercell. The calculated conduction band-edge energy E_c^{RT} and E_c^{LT} , with respect to the top of the valence band, and the fraction of GaAs conduction band in the alloy state, f_Γ^{RT} and f_Γ^{LT} , are given for room temperature and for low temperature (30 K), respectively. Numbers in parentheses after each value give the standard deviation of the last digit(s), as discussed in Appendix B.

$x(\%)$	N_a	E_c^{RT} (eV)	E_c^{LT} (eV)	f_Γ^{RT}	f_Γ^{LT}
0.1	9860780	1.402	1.492	0.927(3)	0.537(66)
0.36	2107392	1.364(1)	1.440(1)	0.805(9)	0.427(63)
0.5	1500000	1.347(1)	1.422(1)	0.585(80)	0.422(52)
1.2	658464	1.269(2)	1.345(2)	0.557(53)	0.584(52)
2.0	393216	1.205(2)	1.275(2)	0.406(66)	0.515(27)

It is of interest to note that, although the form of the integrand is essentially identical to that in the corresponding 3D expressions, the temperature (or typical speed of the particles) does not appear explicitly in the 2D mobility. This reflects the fact that the 2D density of states is constant within the band, leading to an energy-independent scattering rate near the band edge.

III. RESULTS

We have implemented the numerical approach, described in Sec. II. Here, we present results of mobility calculations for a representative range of nitrogen substitutional concentrations: 0.1, 0.36, 0.5, 1.2, and 2% substitutional nitrogen on arsenic sites. Shown in Table I is the size of supercell used in the calculation for each value of the nitrogen concentration x . The supercell sizes were chosen to allow a distribution of between 7,000 and 10,000 N atoms in the calculation. The number of N atoms in each case was chosen to ensure a convergence in the fraction of key N states; the larger number of N atoms used, for instance, for $x=0.1\%$ was chosen to get a representative distribution of N-N pair states, because these states lie very close to the low temperature alloy conduction band minimum at this composition.^{7,20} An analysis of the statistical errors in the relevant physical quantities for each supercell, shown in Table I, is given in Appendix B.

Each group V site in the supercell is occupied with an As or N atom at random, with probability $P(N)=x$ of finding a N atom on any given site. The LCINS basis states are then constructed: one for each N which does not have second-nearest-neighbor nitrogen atoms, and one for each N-N group which share a Ga nearest neighbor, as described in Sec. II A. Their interaction matrix elements between each other and with the GaAs conduction band are calculated from the atomic tight-binding representation of the states to determine the Hamiltonian H^{red} . The calculated (bulk) alloy conduction band edge energy E_c and fraction f_Γ of the GaAs conduction band in the calculated alloy band minimum (at room temperature, $T=300$ K, and at $T=30$ K) are also shown in Table I. (Energy levels are given with reference to the valence band edge.) The bare GaAs conduction band edge is assumed to have its usual temperature dependence,

giving rise to a 90 meV decrease in the bare level between $T=30$ and 300 K. (This change in energies is incorporated in the model by having temperature-dependent tight-binding parameters.) Within the parameterized tight-binding model, the localized levels decrease by 36 meV for the same change in temperature. The interaction matrix elements $\beta_i/\sqrt{N_a}$ are assumed to be independent of temperature.

The observed trends in the variation of f_Γ in Table I may at first appear counterintuitive, with f_Γ at low T , for instance, initially decreasing with composition and then increasing again at higher x . This variation reflects the strong influence of N cluster states which lie close to the alloy band edge. This effect is confirmed by a recent combined theoretical and experimental study of the low temperature effective mass in a wide range of GaNAs samples.²⁰ The measured effective mass was observed to increase when the band edge was approximately degenerate with either of two sets of defect-related levels observed independently in photoluminescence measurements. The increased mass was then quantitatively explained in terms of the reduction in f_Γ due to hybridization of the band edge with these N-related defect levels.

Figure 1 shows the density of states for localized LCINS states $|N_j\rangle$, weighted by β^2/N_a for each state, the square of its interaction matrix element with the conduction band edge. The spectra are shown using the room temperature tight-binding parameters for the supercells listed in Table I. The low temperature spectra are obtained by a rigid shift of the room temperature spectra by 36 meV to higher energies. As the N concentration x is increased from 0.1% to 2%, we see the spectrum evolve from a single peak at energy 1.66 eV (associated with the isolated nitrogen level of the ultradilute limit) to a number of broader peaks, associated with N-N pairs (peak energies at 1.4–1.45 eV and 1.55–1.6 eV, depending on x) and, ultimately, rare larger cluster states (1.2–1.4 eV). We note that the cluster states, which form close to the conduction band edge E_c , hybridize strongly with the conduction band, substantially reducing the value of f_Γ , compared with that obtained in the simple two-band, band anticrossing model.

The room temperature conduction band scattering rate $R(E)$, as discussed in Sec. II D, is shown in Fig. 2 for bulk GaNAs alloys. We note that the scattering rate increases strongly near the isolated N level energy (1.65–1.7 eV above

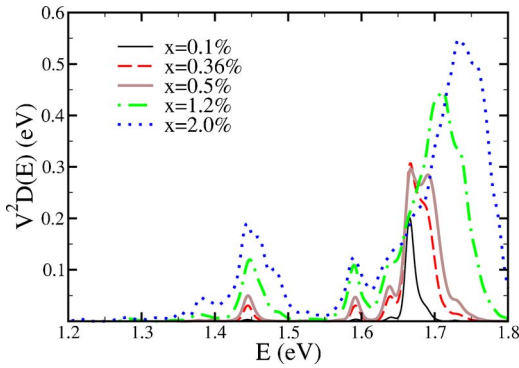


FIG. 1. (Color online) The density of states for localized LCINS states, weighted by β^2/N_a , the square of the interaction matrix element with the GaAs conduction band-edge state, for each state vs energy (referred to the valence band edge at room temperature). Each curve refers to a different nitrogen concentration, x , with $x=0.1\%$, 0.36% , 0.5% , 1.2% , and 2.0% . To smooth the spectra, each energy level is broadened to a Gaussian of width 5 meV.

the valence band edge in Fig. 1) and also near the energy of the localized state associated with N-N pairs (1.4–1.45 eV above the valence band edge in Fig. 1). To find the conductivity for a given carrier concentration, the inverse of this scattering rate is integrated over the appropriately weighted thermal distribution, as given in Eq. (24). From this we find the room temperature carrier mobility, as shown in Fig. 3, varying the chemical potential E_F from $E_c - 5kT$ to $E_c + 5kT$, equivalent to a maximum n -type carrier concentration of about $5 \times 10^{18} \text{ cm}^{-3}$. Here, we have neglected the effect of other scattering mechanisms on the mobility. Assuming that the phonon scattering rate is approximately the same as in pure GaAs,⁴¹ where the room temperature mobility is approximately $8000 \text{ cm}^2(\text{V s})^{-1}$, inclusion of this additional carrier scattering would give rise to a reduction of approximately 30% in the mobility for 0.1% nitrogen concentration and a reduction of 10% or less for the higher nitrogen concentrations.

We note that the final calculated mobility arises not only from the total density of scattering centers, but also from the positioning of the Fermi level relative to the localized state

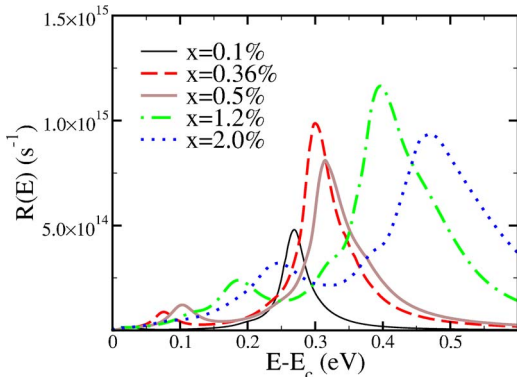


FIG. 2. (Color online) The carrier scattering rate vs energy for nitrogen concentrations, $x=0.1\%$, 0.36% , 0.5% , 1.2% , and 2.0% . The carrier energy is referred to the conduction band edge $E_c(x)$ at room temperature.

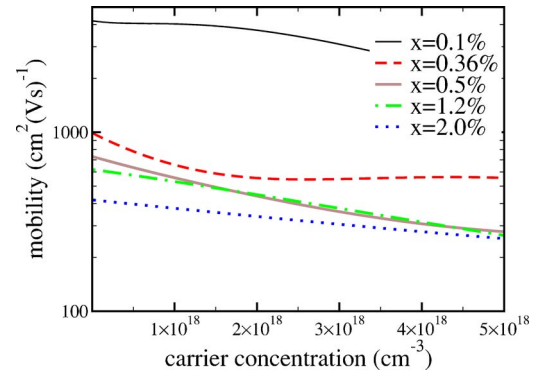


FIG. 3. (Color online) The calculated room temperature n -type carrier mobility vs carrier concentration for various nitrogen concentrations, $x=0.1\%$, 0.36% , 0.5% , 1.2% , and 2.0% .

energy spectrum. Since the localized state spectrum and the position of the conduction band edge change substantially with nitrogen concentration, the mobility may not necessarily increase when the nitrogen concentration decreases, as seen in Fig. 3. For example, at a carrier concentration of $3 \times 10^{18} \text{ cm}^{-3}$, the Fermi level lies about 55 meV above the conduction band edge E_c . Near this energy, we can see from Fig. 2 that the carrier scattering rate for a nitrogen concentration $x=0.5\%$ is slightly greater than that for $x=1.2\%$. This leads, somewhat paradoxically, to a slightly lower mobility for the lower nitrogen concentration.

The calculated mobility as a function of carrier concentration at $T=30 \text{ K}$ is shown in Fig. 4, varying the chemical potential E_F from $E_c - 5kT$ to $E_c + 5kT$, equivalent in this case to a maximum n -type carrier concentration of about $2.5 \times 10^{17} \text{ cm}^{-3}$. Temperature effects on the mobility arise both from changes in the thermal distribution of carriers within the conduction band and due to changes in the relative position of the band edge within the spectrum of nitrogen-induced localized states.

To illustrate the effects of quantum well confinement on the mobility, we have calculated the mobility, $\mu_{QW} = j_{QW}/(e\mathcal{E}n_{QW})$, from Eqs. (30) and (31) or a quantum well of thickness $d=10 \text{ nm}$. Results for room temperature and $T=30 \text{ K}$ are shown in Figs. 5 and 6, respectively. The spec-

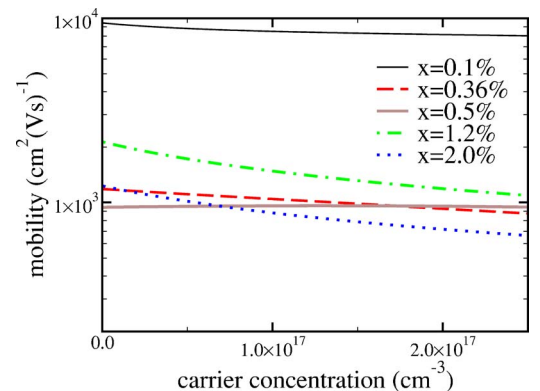


FIG. 4. (Color online) The calculated n -type carrier mobility, at temperature 30 K, vs carrier concentration for various nitrogen concentrations, $x=0.1\%$, 0.36% , 0.5% , 1.2% , and 2.0% .

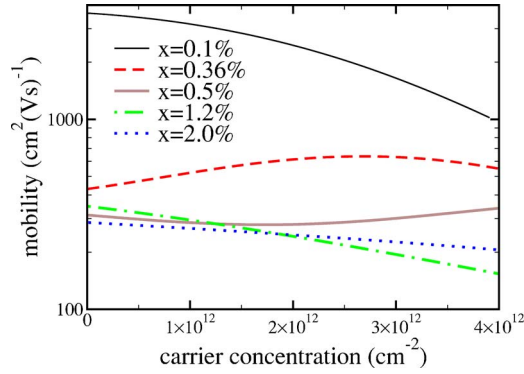


FIG. 5. (Color online) The calculated room temperature n -type carrier mobility for a 10 nm quantum well vs carrier concentration for various nitrogen concentrations, $x=0.1\%$, 0.36% , 0.5% , 1.2% , and 2.0% .

trum of localized states used for each nitrogen concentration is the same as in the 3D calculations. The conduction band edge is shifted by the confinement energy dE , as given in Eq. (15).

IV. DISCUSSION AND CONCLUSIONS

We discuss in detail below the comparison between our calculated values and various measurements of the carrier mobility. In certain cases, good agreement with the measured mobility is found. However, our predicted mobilities are usually somewhat higher than those measured to date, indicating that other scattering mechanisms play a substantial (but not overwhelming) role in limiting the n -type mobility of $\text{GaN}_x\text{As}_{1-x}$. Quantitative comparison with the quantum well samples is difficult because the shift in the band edge due to transverse confinement gives rise to a substantial change in the mobility for higher nitrogen content. Intersubband scattering at higher carrier concentrations in thick quantum wells should give results intermediate between bulk values and those given for occupation of the lowest subband only.

It should also be noted that there can be substantial scatter in the measured mobility between what appear to be closely

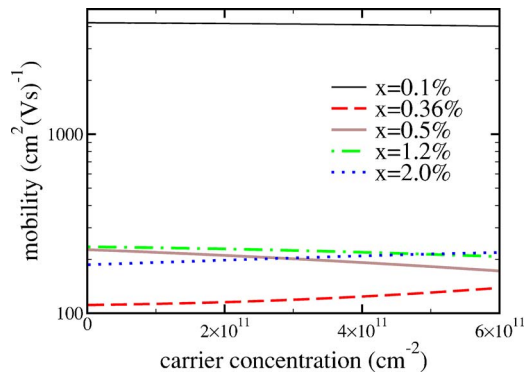


FIG. 6. (Color online) The calculated n -type carrier mobility, at temperature 30 K, for a 10 nm quantum well vs carrier concentration for various nitrogen concentrations, $x=0.1\%$, 0.36% , 0.5% , 1.2% , and 2.0% .

related samples, with, for example,⁹ $\mu=262 \text{ cm}^2(\text{V s})^{-1}$ in a highly doped bulk sample with $x=0.1\%$ and $n=5 \times 10^{18} \text{ cm}^{-3}$, compared¹¹ to $\mu \approx 1500 \text{ cm}^2(\text{V s})^{-1}$ in a $x=0.1\%$ quantum well sample with a density equivalent to a bulk value of $n \approx 4 \times 10^{17} \text{ cm}^{-3}$. This variation emphasizes that factors not considered here are likely to limit the mobility in some experimental studies. It is nevertheless instructive to analyze how the mobilities predicted using the model presented here compare in general with experiment.

Skierbiszewski *et al.*¹³ have reported a mobility of $400 \text{ cm}^2(\text{V s})^{-1}$ at a low carrier concentration of $1.6 \times 10^{17} \text{ cm}^{-3}$ for Si doped $\text{GaN}_{0.014}\text{As}_{0.986}$. From the values shown in Fig. 3, by linear interpolation between the calculated values for $x=1.2\%$ and 2.0% , we obtain a theoretical value of $565 \text{ cm}^2(\text{V s})^{-1}$ for this nitrogen concentration, in good agreement with the measured value.

Young *et al.*⁹ have measured the mobility of Se doped $\text{GaN}_x\text{As}_{1-x}$ for several values of x between 0.01% and 1.3% for higher carrier concentrations of approximately $5 \times 10^{18} \text{ cm}^{-3}$. Their measured value for nitrogen content $x=0.1\%$ is $262 \text{ cm}^2(\text{V s})^{-1}$, considerably lower than our theoretical value of $2200 \text{ cm}^2(\text{V s})^{-1}$ at this carrier concentration. At $x=0.4\%$, their measured value is $187 \text{ cm}^2(\text{V s})^{-1}$, compared to our theoretical value of $385 \text{ cm}^2(\text{V s})^{-1}$ (linear interpolation between values at $x=0.36$ and $x=0.5$).

Mouillet *et al.*¹⁰ have measured mobilities in 2D quantum well structures, with a $\text{GaN}_x\text{As}_{1-x}$ layer thickness of 50 nm and carrier concentration of approximately $1 \times 10^{12} \text{ cm}^{-2}$. They measure room temperature mobilities between $200 \text{ cm}^2(\text{V s})^{-1}$ for $x=0.6\%$ and $600 \text{ cm}^2(\text{V s})^{-1}$ for $x=0.12\%$. The value for $x=0.12\%$ nitrogen content is substantially lower than our predicted value of $3000 \text{ cm}^2(\text{V s})^{-1}$ for a 10 nm quantum well but the mobility for $x=0.6\%$ is in good agreement with our estimate of $270 \text{ cm}^2(\text{V s})^{-1}$. At low temperature, our theoretical mobility ($T=30 \text{ K}$) for 0.1% nitrogen is $3500 \text{ cm}^2(\text{V s})^{-1}$, approximately four times larger than their measured value of $800 \text{ cm}^2(\text{V s})^{-1}$ for 0.12% nitrogen, while our value of the mobility for higher nitrogen content is approximately $150 \text{ cm}^2(\text{V s})^{-1}$ (see Fig. 6), in good agreement with the measured value of approximately $120 \text{ cm}^2(\text{V s})^{-1}$ for $x=0.6\%$.

Fowler *et al.*¹¹ have measured mobilities in 2D quantum well structures, with a $\text{GaN}_x\text{As}_{1-x}$ layer thickness of 13 nm and carrier concentration of approximately $5 \times 10^{11} \text{ cm}^{-2}$, for nitrogen content, $x=0.1\%$ and 0.4% at low temperature and room temperature. For $x=0.1\%$, they obtain mobility values of $1500\text{--}2000 \text{ cm}^2(\text{V s})^{-1}$ (with a weak temperature dependence), somewhat lower than our calculated values of 3460 and $4070 \text{ cm}^2(\text{V s})^{-1}$ for $T=300$ and 30 K , respectively. For $x=0.4\%$, they obtain mobility values of $300\text{--}400 \text{ cm}^2(\text{V s})^{-1}$ (with a weak temperature dependence), somewhat higher than our calculated values of 250 and $150 \text{ cm}^2(\text{V s})^{-1}$ for $T=300$ and 30 K , respectively.

In Ref. 13, Skierbiszewski *et al.* have pointed to the increase of the effective mass as a primary source of reduced mobility in the dilute nitrides. Indeed, the expression in Eq. (28) appears to have a strong mass-dependence (m^*)^{-5/2}, which would support this interpretation. However, recall that the increase in mass in the conduction band has been

shown^{7,20} to be primarily due to the reduction of the fraction, f_Γ , of the pure GaAs conduction band in the alloy conduction band states, arising from hybridization with the localized nitrogen-related states. The interaction matrix element $(\beta')^2$ is scaled by this same factor f_Γ , so that the term β'^4 in Eq. (28) has a counterbalancing $(m^*)^{-2}$ dependence, leaving a much weaker $1/\sqrt{m^*}$ dependence of the mobility. (E_i and Γ_i are approximately independent of m^* .) Our analysis has assumed parabolic bands. Given the rather weak mass dependence of the carrier scattering rate, we expect this to give reasonable results for the mobility although the mass may in fact have a substantial energy dependence.

As discussed in Sec. II D, the scattering rate calculated in the resonant scattering approach by isolated nitrogen states is the same as the imaginary part of the self-energy in the CPA (scaled by $2/\hbar$). For carrier concentrations in excess of 10^{19} cm^{-3} , the Fermi level is close to the energy peak of the isolated nitrogen state in the density of localized states. The scattering of carriers is then dominated by isolated nitrogen scattering and the CPA (or the approach of Ref. 6) gives mobilities close to experimentally measured values.²² The inclusion of scattering of carriers near the conduction band edge by the entire spectrum of localized states in the present approach is physically equivalent^{6,24} to the introduction in Ref. 22 of scattering by random variations in the band edge as a term separate from the scattering due to isolated nitrogen states (CPA conduction band broadening). At low carrier concentrations, the random potential scattering dominates over the CPA conduction band broadening (see Fig. 4 of Ref. 22), in agreement with our results, showing the dominance of nitrogen cluster scattering for carriers near the conduction band edge.

The physical model of elastic scattering of extended carrier states is open to question at very low carrier concentration, where the occupied states may be primarily below the mobility edge. Indeed, calculations of states in an effective mass model in the presence of a disordered random potential, corresponding²⁴ to a room temperature mobility of $150 \text{ cm}^2(\text{V s})^{-1}$, suggest that the states at energies within 20 meV of the conduction band edge are localized by disorder.⁴⁴ Even in the high carrier concentration regime, the carrier scattering rate is sufficiently high when the nitrogen concentration is of the order of 1% to make the nominal carrier mean-free-path $l = v/R(E)$ as short as 5 nm. The energy-dependence of the mean-free-path is shown in Fig. 7 for various nitrogen concentrations. For this very short mean-free-path, the wave-packet scattering picture, which is implicit in the Boltzmann transport equation, may start to break down, although it should still provide a reasonable estimate of the particle current in the presence of an electric field.

Nevertheless, the analysis given here clearly indicates that the mobility in dilute nitride samples is predominantly limited by nitrogen pair and cluster states near the conduction band edge. If these states could be removed or shifted to energies further away from the conduction band edge (e.g., by alloying or by the application of pressure), then the mobility would be primarily determined by scattering from the isolated nitrogen peak. Previous calculations⁶ indicate that

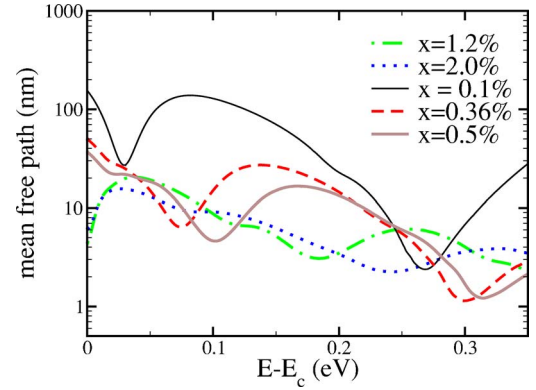


FIG. 7. (Color online) The calculated n -type carrier mean-free-path l vs energy for nitrogen concentrations, $x=0.1\%$, 0.36% , 0.5% , 1.2% , and 2.0% . The carrier energy is referred to as the conduction band edge $E_c(x)$.

this would give rise to a mobility of the order of $1000 \text{ cm}^2(\text{V s})^{-1}$. We note that this does not take into account scattering from charge traps associated with interstitial nitrogen incorporation,²⁶ which may be a substantial source of further scattering in the material.

In summary, we have calculated the energy-dependent scattering rate of n -type carriers in the dilute nitride $\text{GaN}_x\text{As}_{1-x}$ due to resonant interaction with nitrogen-induced localized states in the material, for several nitrogen concentrations between 0.1% and 2%. The scattering rates are used in the Boltzmann transport equation to find the n -type mobility in the relaxation time approximation. The resulting mobilities are in the range of $300\text{--}500 \text{ cm}^2(\text{V s})^{-1}$ for nitrogen concentrations of the order of 1% and carrier concentrations in the range $(0\text{--}5) \times 10^{18} \text{ cm}^{-3}$, in reasonable agreement with measured values. We find that scattering by states associated with substitutional nitrogen pairs and other, more complex nitrogen clusters play a major role in reducing the mobility in these alloys.

ACKNOWLEDGMENTS

This work has been supported by Science Foundation Ireland. S. F. wishes to thank S. Baranovskii, R. Goldman, and C. Kurdak for useful discussions and the FOCUS Center at the University of Michigan for hospitality during part of this work.

APPENDIX A: RESONANCE SUM RULES

In this appendix, we give details of the sum rules which are used to determine the peak shift $E_N - E'_N$ and linewidth Γ for a localized state interacting with a continuum band. For the model Hamiltonian, $H_0 + \Delta H$, specified in Eqs. (6) and (7) we have that

$$\sum_{p'} |\langle p' | N \rangle|^2 = \langle N | N \rangle = 1, \quad (\text{A1})$$

and

$$\sum_{p'} E(p') |\langle p' | N \rangle|^2 = \langle N | H_0 + \Delta H | N \rangle = E_N, \quad (\text{A2})$$

where $|p'\rangle$ are the exact eigenstates of $H_0 + \Delta H$. Defining $W(E) = |\langle p' | N \rangle|^2$, where $E = \langle p' | H_0 + \Delta H | p' \rangle = E(p')$, we find the normalization sum rule,

$$\int W(E) D(E) dE = 1, \quad (\text{A3})$$

and the energy sum rule

$$\int W(E) E D(E) dE = E_N, \quad (\text{A4})$$

where $D(E)$ is the density of states $|p'\rangle$. For weak interaction and a slowly varying density of states, we may take $D(E)$ to be a constant over the range of energies where $W(E)$ is substantial. Assuming the Lorentzian line shape for $W(E)$, given in Eq. (10), we find that $C = \beta^2 / N_a$ satisfies the normalization sum rule, Eq. (A3). This value of C also gives the correct value of $W(E)$ for energies E far from E_N ; using first order perturbation theory, the change in the state $|p\rangle$ at energies far from E_N is

$$\langle N | p' \rangle = \langle N | \Delta H | p \rangle / [E(p) - E_N] = \frac{\beta \sqrt{N_a}}{E(p) - E_N}. \quad (\text{A5})$$

The difference $E_N - E'_N$ satisfies the equation

$$E_N - E'_N = \int \frac{[E(p') - E'_N] \beta^2 / N_a}{[E(p') - E'_N]^2 + (\Gamma/2)^2} D(E) dE, \quad (\text{A6})$$

which reduces approximately to the second order perturbation theory shift:

$$dE_N = \int \frac{|\langle p | \Delta H | N \rangle|^2}{E_N - E(p)} D(E) dE. \quad (\text{A7})$$

This shift in energy is affected by the maximum energy E_{\max} at which the coupling β of the localized state $|N\rangle$ to the conduction band is nonzero. For E_N near the conduction band minimum, the bulk energy shift is

$$dE = \frac{E_0}{8\pi^2} \left(\frac{\beta}{E_0} \right)^2 \sqrt{\frac{E_{\max} - E_c}{E_0}}. \quad (\text{A8})$$

In keeping with the limitation of the effective mass description of the GaAs conduction bands away from the Γ -point in the Brillouin zone and the fact that the localized state $|N\rangle$ is generated in the LCINS representation to include the mixing of states in energy above the L-point in the GaAs conduction bands, we set E_{\max} less than the energy of the conduction band at the L-point. In practice, the calculated values of the mobility are only slightly affected by the shift $E_N - E'_N$ in the localized state resonance. We set $E_{\max} = E_c + 230$ meV in all

calculations for bulk and quantum well systems and numerically evaluate the shift $E_N - E'_N$ from the second order perturbation expression in Eq. (A7).

When the density of states changes substantially within the resonance peak associated with the localized state (as it does near the conduction band edge), we still approximate $W(E)$ by a Lorentzian [Eq. (10)]. We keep the numerator $C = \beta^2 / N_a$, since it gives the correct behavior for large values of $|E - E_N|$ and adjust Γ so that the weight sum rule, Eq. (A3), is satisfied.

The discussion so far assumes that a bound state is not formed. If E'_N is less than the conduction band minimum E_c , a bound state will be formed and the weight sum rule is modified. In that case, a reasonable approximation is to set $\Gamma = 0$ in the expression for the spectral weight since no conduction band states have energies near E'_N .

APPENDIX B: VARIANCE OF E_c AND f_Γ

Here we present an analysis of the statistical variance in the alloy conduction band minimum, calculated in large supercells with random nitrogen substitutions (see Table I). The energy E_c of this state is found by diagonalization of the reduced Hamiltonian H_{red} , defined in Eqs. (3) and (4) and the GaAs conduction band weight f_Γ is defined in Eq. (21). The addition (or removal) of a single localized state, with energy E_j and interaction matrix element with the GaAs conduction band $\beta_j / \sqrt{N_a}$, in a large supercell will cause a small change in E_c and f_Γ . Treating the coupling of the additional localized state to the alloy conduction band state as a two-level problem, we find these changes as

$$\delta E_{c,j} = \sqrt{\Delta^2 + f_\Gamma \beta_j^2 / N_a} - \Delta \quad (\text{B1})$$

and

$$\frac{\delta f_{\Gamma,j}}{f_\Gamma} = \frac{f_\Gamma \beta_j^2 / N_a}{f_\Gamma \beta_j^2 / N_a + [\sqrt{\Delta^2 + f_\Gamma \beta_j^2 / N_a} + \Delta]^2}, \quad (\text{B2})$$

where $\Delta = |E_j - E_c|/2$. We now assume that, for likely variations in the distribution of localized states, each localized state gives a statistically independent contribution to the shift of the alloy conduction band state. Thus the variance of the numerically calculated E_c is

$$\langle \delta E^2 \rangle = \sum_j |\delta E_{c,j}|^2 \quad (\text{B3})$$

and the variance of $\ln f_\Gamma$ is

$$\langle (\delta \ln f_\Gamma)^2 \rangle = \sum_j \left| \frac{\delta f_{\Gamma,j}}{f_\Gamma} \right|^2, \quad (\text{B4})$$

where j is summed over the localized states in the supercell. We note that states close in energy to E_c make a large contribution to the variance of E_c and (even more so) of f_Γ .

- *Present address: Laboratoire CRISMAT, UMR CNRS-ENSICAEN (ISMRA) 6508, 6 Boulevard Maréchal Juin, 14050 Caen Cedex, France.
- ¹H. Reichert, A. Ramakrishnan, and G. Steinle, *Semicond. Sci. Technol.* **17**, 892 (2002).
 - ²J. S. Harris, *Semicond. Sci. Technol.* **17**, 880 (2002).
 - ³J. F. Geisz and D. J. Friedman, *Semicond. Sci. Technol.* **17**, 769 (2002).
 - ⁴P. R. C. Kent and A. Zunger, *Phys. Rev. B* **64**, 115208 (2001).
 - ⁵P. R. C. Kent, L. Bellaiche, and A. Zunger, *Semicond. Sci. Technol.* **17**, 851 (2002).
 - ⁶S. Fahy and E. P. O'Reilly, *Appl. Phys. Lett.* **83**, 3731 (2003).
 - ⁷A. Lindsay and E. P. O'Reilly, *Phys. Rev. Lett.* **93**, 196402 (2004).
 - ⁸M. Weyers, M. Sato, and H. Ando, *Jpn. J. Appl. Phys., Part 2* **31**, L853 (1992).
 - ⁹D. L. Young, J. F. Geisz, and T. J. Coutts, *Appl. Phys. Lett.* **82**, 1236 (2003).
 - ¹⁰R. Mouillet, L. de Vaulchier, E. Delporte, Y. Guldner, L. Travers, and J.-C. Harmand, *Solid State Commun.* **126**, 333 (2003).
 - ¹¹D. Fowler, O. Makarovskiy, A. Patanè, L. Eaves, L. Geelhaar, and H. Riechert, *Phys. Rev. B* **69**, 153305 (2003).
 - ¹²A. J. Ptak, S. W. Johnston, S. Kurtz, D. J. Reideman, and W. K. Metzger, *J. Cryst. Growth* **251**, 392 (2004).
 - ¹³C. Skierbiszewski, P. Perlin, P. Wisniewski, T. Suski, W. Walukiewicz, W. Shan, J. W. Ager, E. E. Haller, J. F. Geisz, D. J. Friedman, J. M. Olson, and S. R. Kurtz, *Phys. Status Solidi B* **216**, 135 (1999).
 - ¹⁴K. Volz, J. Koch, B. Kunert, and W. Stolz, *J. Cryst. Growth* **248**, 451 (2003).
 - ¹⁵W. Shan, W. Walukiewicz, J. W. Ager III, E. E. Haller, J. F. Geisz, D. J. Friedman, J. M. Olson, and S. R. Kurtz, *Phys. Rev. Lett.* **82**, 1221 (1999).
 - ¹⁶H. P. Hjalmarson, P. Vogl, D. J. Wolford, and J. D. Dow, *Phys. Rev. Lett.* **44**, 810 (1980).
 - ¹⁷X. Liu, M.-E. Pistol, L. Samuelson, S. Schwetlick, and W. Siefert, *Appl. Phys. Lett.* **56**, 1451 (1990).
 - ¹⁸L. Bellaiche, S.-H. Wei, and A. Zunger, *Phys. Rev. B* **54**, 17568 (1996).
 - ¹⁹E. P. O'Reilly, A. Lindsay, A. Tomić, and M. Kamal-Saadi, *Semicond. Sci. Technol.* **17**, 870 (2002).
 - ²⁰F. Masia, G. Pettinari, A. Polimeni, M. Felici, A. Miriametro, M. Capizzi, A. Lindsay, S. B. Healy, E. P. O'Reilly, A. Cristofoli, G. Bais, M. Piccin, S. Rubini, F. Martelli, A. Franciosi, P. J. Klar, K. Volz, and W. Stolz, *Phys. Rev. B* **73**, 073201 (2006).
 - ²¹O. F. Sankey, J. D. Dow, and K. Hess, *Appl. Phys. Lett.* **41**, 664 (1982).
 - ²²J. Wu, K. M. Yu, and W. Walukiewicz, *IEE Proc.: Optoelectron.* **151**, 460 (2004).
 - ²³S. Fahy, A. Lindsay, and E. P. O'Reilly, *IEE Proc.: Optoelectron.* **151**, 352 (2004).
 - ²⁴A. L. Efros and M. E. Raikh, *Optical Properties of Mixed Crystals* (Elsevier, Amsterdam, 1988).
 - ²⁵M. A. Fisher, A. R. Adams, E. P. O'Reilly, and J. J. Harris, *Phys. Rev. Lett.* **59**, 2341 (1987).
 - ²⁶S. B. Zhang and S.-H. Wei, *Phys. Rev. Lett.* **86**, 1789 (2001).
 - ²⁷S. B. Zhang, A. Janotti, S.-H. Wei, and C. G. V. de Walle, *IEE Proc.: Optoelectron.* **151**, 369 (2004).
 - ²⁸A. Lindsay and E. P. O'Reilly, *Solid State Commun.* **118**, 313 (2001).
 - ²⁹A. Lindsay and E. P. O'Reilly, *Physica E (Amsterdam)* **21**, 901 (2004).
 - ³⁰J. Endicott, A. Patane, J. Ibanez, L. Eaves, M. Bissiri, M. Hopkinson, R. Airey, and G. Hill, *Phys. Rev. Lett.* **91**, 126802 (2003).
 - ³¹A. Lindsay, S. Tomić, and E. P. O'Reilly, *Solid-State Electron.* **47**, 443 (2003).
 - ³²A. Lindsay and E. P. O'Reilly, *Solid State Commun.* **112**, 443 (1999).
 - ³³D. R. Hamann, M. Schluter, and C. Chiang, *Phys. Rev. Lett.* **43**, 1494 (1979).
 - ³⁴J. Wu, W. Shan, and W. Walukiewicz, *Semicond. Sci. Technol.* **17**, 860 (2002).
 - ³⁵H. A. McKay, R. M. Feenstra, T. Schmidling, U. W. Pohl, and J. F. Geisz, *Appl. Phys. Lett.* **78**, 82 (2001).
 - ³⁶A. Patane, J. Endicott, J. Ibanez, P. N. Brunkov, L. Eaves, S. B. Healy, A. Lindsay, E. P. O'Reilly, and M. Hopkinson, *Phys. Rev. B* **71**, 195307 (2005).
 - ³⁷S. Tomić, E. P. O'Reilly, P. J. Klar, H. Gruning, W. Heimbrod, W. M. Chen, and I. A. Buyanova, *Phys. Rev. B* **69**, 245305 (2004).
 - ³⁸M. Hetterich, A. Grau, A. Y. Egorov, and H. Riechert, *J. Phys.: Condens. Matter* **16**, S3151 (2004).
 - ³⁹J. J. Sakurai, *Modern Quantum Mechanics* (Addison-Wesley, Reading, MA, 1994).
 - ⁴⁰P. Yu and M. Cardona, *Fundamentals of Semiconductors* (Springer, Berlin, 2001).
 - ⁴¹W. Walukiewicz, H. E. Ruda, J. Lagowski, and H. C. Gatos, *Phys. Rev. B* **30**, 4571 (1984).
 - ⁴²See special journal issues on dilute nitrides: *Semicond. Sci. Technol.* **17**(8), edited by J. Ager and W. Walukiewicz (2002) and *Semicond. Sci. Technol.* **151**(5), edited by E. P. O'Reilly, N. Balkan, I. A. Buyanova, X. Marie, and H. Reichert (2004).
 - ⁴³The average of the scattering rate [Eq. (16)] for uniformly distributed scattering centers across the well is approximately, but not exactly, equal to the scattering rate [Eq. (18)] for the average of $\Psi(z)^4$ and average of Γ^2 . The error arises principally from the values of z where $\Psi(z) \rightarrow 0$. However, this error is small and is substantially reduced if one includes the penetration of Ψ into the barrier region, as occurs in the exact quantum well wave functions.
 - ⁴⁴D. McPeake, I. Bosa, A. Lindsay, and S. Fahy (unpublished).